

PHYSICAL REVIEW A

GENERAL PHYSICS

THIRD SERIES, VOLUME 31, NUMBER 5

MAY 1985

Ab initio calculation of $4f^N 6s^2$ hyperfine structure in neutral rare-earth atoms

K. T. Cheng and W. J. Childs

Argonne National Laboratory, Argonne, Illinois 60439

(Received 19 November 1984)

The multiconfiguration Dirac-Fock (MCDF) method is used to calculate excitation energies, Landé g values, and hyperfine-structure (hfs) constants for the lowest multiplets of the $4f^N 6s^2$ configurations of neutral rare-earth atoms. Although no adjustable parameters are used, the results are in rather good agreement with experiment. The calculated excitation energies and dipole hfs constants (using the known moment values) differ from experiment by typically 5%, and the g values by 0.1%. Relative to quadrupole moment values determined from muonic-atom hfs or Coulomb excitation, the calculated electric-quadrupole hfs is typically $(30 \pm 2)\%$ too large, consistent with a Sternheimer shielding factor (not included in the MCDF calculations) of $R_{4f} = +0.23$. The calculated J dependence for all four observables is generally in good agreement with experiment for the ground multiplets. Particular cases where the MCDF results are less accurate are identified and discussed.

I. INTRODUCTION

The fine and hyperfine structure (hfs) of the neutral rare-earth elements have been studied with a variety of techniques over the years. Among the more fruitful of these have been the traditional methods of optical and radio-frequency (rf) spectroscopy,¹ and more recently, high-resolution laser spectroscopy.² Within the last few years the latter two techniques have been combined in the atomic-beam laser-rf double-resonance technique,³ which is capable of both extremely high sensitivity and resolution.

Although a number of electron configurations lie low in the neutral rare earths, for simplicity we will limit ourselves in this study to the $4f^N 6s^2$ configurations which give rise to the ground and lowest excited states in most of these atoms.⁴ Because of the substantial separation of the ground multiplet from other terms of the same parity, the lowest levels are normally rather close to the L - S coupling limit. Since only one electron shell ($4f$) is open, one would expect the hfs to be relatively simple to interpret, at least qualitatively.

Two main approaches may be used in attempting to understand systematically the substantial amount of fine- and hyperfine-structure data now available for the low-lying terms of the $4f^N 6s^2$ configurations. The first method may be called the semiempirical or adjustable-parameter method.⁵ In this approach numerical eigenvectors are obtained for the states of interest from least-squares multiparameter fits to the experimental fine-structure energy separations. The composition of each

state is thereby described in terms of a linear combination of the states of the L - S configuration under consideration. The hyperfine interaction is then treated as a first-order perturbation according to the effective operator method,⁶ and for each state the eigenvector is used to evaluate the expectation values of the hyperfine operators, treating the individual interaction strengths as adjustable parameters. This now classical method has been used for many years in the analysis of hfs.^{7,8} It has the virtue that the hfs splittings can be predicted for as yet unstudied states with surprising accuracy. The disadvantage is clearly a less-than-rigorous understanding of the physical details of the interactions.

The second approach to understanding the observed hfs is to calculate it from first principles and then to try to learn from any differences with experiment. As hyperfine interactions are sensitive to electron correlations as well as to relativity, atomic hfs provides important tests for *ab initio* atomic-structure theory. For light atoms where relativistic effects are weak, the configuration interaction (CI) method⁹ and the diagrammatic many-body perturbation theory (MBPT) (Ref. 10) have been successful in studying atomic hfs. For heavy atoms such as the rare earths, there are hardly any *ab initio* hfs calculations reported to date. Instead, the usual approach is to calculate the hfs radial parameters with the configuration-average Dirac-Fock (DF) method and then to compare them with those obtained from the semiempirical effective-operator method mentioned above.⁷

In this work the multiconfiguration Dirac-Fock (MCDF) method is used to study the $4f^N 6s^2$ hfs in neu-

tral rare-earth atoms. The MCDF method is a relativistic self-consistent-field calculation which is, in principle, applicable to any atom regardless of its size. Also, electron correlations can be taken into account by including the dominant configurations in the calculations. We shall restrict ourselves to first-order hyperfine interactions in this study. Thus, in calculating the hfs, the distortions of the electron shell by nuclear moments (e.g., the Sternheimer shielding)¹¹ are not included in the calculations.

It is important in assessing the success of an atomic-structure theory to test it on several observables since each is sensitive to different types of configurations and different features of the wave functions. The observables chosen for comparison with the MCDF theory are the excitation energy E , the Landé g value g_J , the magnetic dipole hfs constant A , and the electric-quadrupole hfs constant B . These quantities have been measured precisely for a large number of low-lying $4f^N 6s^2$ levels of the neutral rare earths. The atomic-beam magnetic-resonance technique used in a large number of early measurements¹ of hfs and g values has largely been superseded in recent years by the laser-rf double-resonance method.^{2,3} The much greater sensitivity of the newer technique has made it possible to study a number of more highly excited (and consequently less well-populated) metastable levels. This has allowed measurement of the hfs in all members of the ground term for most neutral rare-earth atoms, thereby testing the J dependence of the hfs interactions critically. The newer data are vital for carrying the study through the second half of the $4f$ shell where the much greater statemixing can give the theory a more rigorous testing.

II. THEORY

In this work, MCDF eigenenergies and wave functions are calculated from a program developed by Desclaux.¹² Specifically, the Coulomb interactions between the electrons are included in the self-consistent-field calculations, while corrections for the Breit interactions are treated as first-order perturbations to the total energies. The MCDF wave functions $|JM_J\rangle$ employed here consist of all possible jj -coupled states that arise from the $4f^N 6s^2$ electronic configurations. They are used to form eigenstates $|IJFM_F\rangle$ of the hyperfine Hamiltonian, with \mathbf{I} and \mathbf{J} being the total angular momentum of the nucleus and the electron state, respectively, and $\mathbf{F}=\mathbf{I}+\mathbf{J}$.

A. Hyperfine interaction

The relativistic hyperfine Hamiltonian is given by

$$H_{\text{hfs}} = \sum_k \mathbf{M}^{(k)} \cdot \mathbf{T}^{(k)}, \quad (1)$$

where $\mathbf{M}^{(k)}$ and $\mathbf{T}^{(k)}$ are spherical tensor operators of rank k , representing the nuclear and electronic parts, respectively, of the interaction. In first-order perturbation theory, hyperfine energies $W(J)$ of the fine-structure state $|JM_J\rangle$ are expectation values of H_{hfs} such that

$$\begin{aligned} W(J) &= \langle IJFM_F | \sum_k \mathbf{M}^{(k)} \cdot \mathbf{T}^{(k)} | IJFM_F \rangle \\ &= \sum_k (-1)^{I+J+F} \begin{Bmatrix} I & J & F \\ J & I & k \end{Bmatrix} \\ &\quad \times \langle I || \mathbf{M}^{(k)} || I \rangle \langle J || \mathbf{T}^{(k)} || J \rangle. \end{aligned} \quad (2)$$

In the magnetic dipole case ($k=1$), the nuclear dipole moment μ_I (in units of the nuclear magneton $\mu_N = e\hbar/2m_p c$) is defined as

$$\mu_I \mu_N = \langle II | \mathbf{M}_0^{(1)} | II \rangle = \begin{Bmatrix} I & 1 & I \\ -I & 0 & I \end{Bmatrix} \langle I || \mathbf{M}^{(1)} || I \rangle, \quad (3)$$

while the operator $\mathbf{T}_q^{(1)}$ is given by⁷

$$\mathbf{T}_q^{(1)} = \sum_j t_q^{(1)} = \sum_j -ie\sqrt{8\pi/3}r_j^{-2}\alpha_j \cdot \mathbf{Y}_{1q}^{(0)}(\hat{\mathbf{r}}_j), \quad (4)$$

in which $\alpha = (\frac{0}{\sigma} \sigma)$ is the Dirac matrix, $\mathbf{Y}_{kq}^{(\lambda)}$ represents the vector spherical harmonic,¹³ $e = |e|$ is the magnitude of the electron charge, and the index j refers to the j th electron of the atom. For simplicity, we shall drop the electron index j in subsequent discussions. Defining the magnetic dipole hyperfine constant A by

$$A = \mu_N \left[\frac{\mu_I}{I} \right] \frac{\langle J || \mathbf{T}^{(1)} || J \rangle}{\sqrt{J(J+1)(2J+1)}}, \quad (5)$$

the magnetic dipole hyperfine energy W_{M1} is then given by the familiar formula

$$W_{M1} = A \langle \mathbf{I} \cdot \mathbf{J} \rangle = A K / 2, \quad (6)$$

where $K = F(F+1) - I(I+1) - J(J+1)$.

In the electric-quadrupole case ($k=2$), the nuclear quadrupole moment Q is defined as

$$\frac{eQ}{2} = \langle II | \mathbf{M}_0^{(2)} | II \rangle = \begin{Bmatrix} I & 2 & I \\ -I & 0 & I \end{Bmatrix} \langle I || \mathbf{M}^{(2)} || I \rangle, \quad (7)$$

while the operator $\mathbf{T}_q^{(2)}$ is given by¹²

$$\mathbf{T}_q^{(2)} = \sum_j t_q^{(2)} = \sum_j -er^{-3} \mathbf{C}_q^{(k)}(\hat{\mathbf{r}}). \quad (8)$$

Here, $\mathbf{C}_q^{(k)} = \sqrt{4\pi/(2k+1)} \mathbf{Y}_{kq}$, with \mathbf{Y}_{kq} being a spherical harmonic, and the sum goes through all electrons. Defining the electric-quadrupole hyperfine constant B by

$$B = 2eQ \left[\frac{2J(2J-1)}{(2J+1)(2J+2)(2J+3)} \right]^{1/2} \langle J || \mathbf{T}^{(2)} || J \rangle, \quad (9)$$

the electric-quadrupole hyperfine energy W_{E2} is then given by

$$W_{E2} = \frac{B}{2} \frac{3K(K+1) - 4I(I+1)J(J+1)}{2I(2I-1)2J(2J-1)}. \quad (10)$$

B. Landé g factor

In a homogeneous magnetic field \mathbf{B} , the interaction Hamiltonian is given by

$$H' = \sum e \boldsymbol{\alpha} \cdot \mathbf{A} = \sum e \boldsymbol{\alpha} \cdot \left(\frac{1}{2} \mathbf{B} \times \mathbf{r} \right). \quad (11)$$

In terms of a scalar product of two first-order tensors, we have

$$H' = \frac{1}{2} \mathbf{N} \cdot \mathbf{B}, \quad (12)$$

where¹⁴

$$\mathbf{N}_q^{(1)} = \sum \mu_q^{(1)} = - \sum ie \sqrt{8\pi/3} r \alpha \cdot \mathbf{Y}_{1q}^{(0)}(\hat{\mathbf{r}}). \quad (13)$$

Comparing Eqs. (4) and (13), the similarity between the tensor operators $\mathbf{T}_q^{(1)}$ and $\mathbf{N}_q^{(1)}$ is obvious.

The Landé g factor g_J is defined by the magnetic moment $\boldsymbol{\mu}$ of the atom in state $|JM_J\rangle$ as

$$\boldsymbol{\mu} = -g_J \mu_B \mathbf{J}, \quad (14)$$

with $\mu_B = e\hbar/2mc$ being the Bohr magneton. Since the interaction energy $W = \langle H' \rangle = \langle -\boldsymbol{\mu} \cdot \mathbf{B} \rangle = g_J \mu_B \langle \mathbf{J} \cdot \mathbf{B} \rangle$, one can make use of the projection theorem¹⁵ to show that

$$g_J = \frac{1}{2\mu_B} \frac{\langle J || \mathbf{N}^{(1)} || J \rangle}{\sqrt{J(J+1)(2J+1)}}. \quad (15)$$

Because of the quantum electrodynamic corrections, the electron g factor g_s is not exactly 2 but is

$$g_s = 2 \left[1 + \frac{\alpha}{2\pi} - 0.328 \frac{\alpha^2}{\pi^2} + \dots \right] \approx 2 \times (1.001160). \quad (16)$$

This leads to a correction to the interaction Hamiltonian¹⁶

$$\Delta H' = 0.001160 \mu_B \beta \boldsymbol{\Sigma} \cdot \mathbf{B}, \quad (17)$$

where $\beta = \begin{pmatrix} 0 & 0 \\ 0 & -1 \end{pmatrix}$ and $\boldsymbol{\Sigma} = \begin{pmatrix} \sigma_0^0 \\ 0 \end{pmatrix}$. If we define the operator $\Delta \mathbf{N}_q^{(1)}$ by

$$\Delta \mathbf{N}_q^{(1)} = \sum \Delta \mu_q^{(1)} = \sum \beta \boldsymbol{\Sigma}_q, \quad (18)$$

then the correction to the Landé g factor is given by

$$\Delta g_J = 0.001160 \frac{\langle J || \Delta \mathbf{N}^{(1)} || J \rangle}{\sqrt{J(J+1)(2J+1)}}. \quad (19)$$

C. Radial matrix elements

Angular recoupling programs are set up to reduce the matrix elements $\langle J || \mathbf{T}^{(k)} || J \rangle$ and $\langle J || \mathbf{N}^{(1)} || J \rangle$ to terms that involve single-particle orbitals only. The Dirac wave function for an individual electron is given by

$$|n\kappa m\rangle = \frac{1}{r} \begin{pmatrix} P_{n\kappa}(r) \Omega_{\kappa m}(\hat{\mathbf{r}}) \\ i Q_{n\kappa}(r) \Omega_{-\kappa m}(\hat{\mathbf{r}}) \end{pmatrix}, \quad (20)$$

where n , κ , and m are the principal, angular, and magnetic quantum numbers, respectively. In particular, $\kappa = \mp(j + \frac{1}{2})$ for $j = l \pm \frac{1}{2}$, with l and j being the orbital and total angular momenta of the electron.

The functions P and Q are the large and small components of the radial wave function, while the function

$$\Omega_{\kappa m}(\hat{\mathbf{r}}) = \sum_q C(l \frac{1}{2} j; m - q q m) Y_{lm-q}(\hat{\mathbf{r}}) \chi_q \quad (21)$$

is the electron spinor in the LSJ coupling scheme, with $\chi_q = \begin{pmatrix} 1 \\ 0 \end{pmatrix}$ or $\begin{pmatrix} 0 \\ 1 \end{pmatrix}$ for $q = \frac{1}{2}$ or $-\frac{1}{2}$, respectively. In the following we use atomic units in evaluating matrix elements

and drop the principal quantum number n for simplicity. The reductions of the single-particle matrix elements into angular factors and radial integrals are straightforward. We only show the results here:

$$\langle \kappa m | \mathbf{t}_q^{(1)} | \kappa' m' \rangle = - \langle -\kappa m | \mathbf{C}_q^{(1)} | \kappa' m' \rangle (\kappa + \kappa') [r^{-2}]_{\kappa\kappa'}, \quad (22)$$

$$\langle \kappa m | \mathbf{t}_q^{(2)} | \kappa' m' \rangle = - \langle \kappa m | \mathbf{C}_q^{(2)} | \kappa' m' \rangle \langle r^{-3} \rangle_{\kappa\kappa'}, \quad (23)$$

$$\langle \kappa m | \mu_q^{(1)} | \kappa' m' \rangle = - \langle -\kappa m | \mathbf{C}_q^{(1)} | \kappa' m' \rangle (\kappa + \kappa') [r]_{\kappa\kappa'}, \quad (24)$$

$$\langle \kappa m | \Delta \mu_q^{(1)} | \kappa' m' \rangle = \langle -\kappa m | \mathbf{C}_q^{(1)} | \kappa' m' \rangle (\kappa + \kappa' - 1) \langle r^0 \rangle_{\kappa\kappa'}. \quad (25)$$

The angular functions are given by

$$\langle \kappa m | \mathbf{C}_q^{(k)} | \kappa' m' \rangle = (-1)^{j-m} \begin{pmatrix} j & k & j' \\ -m & q & m' \end{pmatrix} \langle \kappa || \mathbf{C}^{(k)} || \kappa' \rangle, \quad (26)$$

$$\langle \kappa || \mathbf{C}^{(k)} || \kappa' \rangle = (-1)^{j+1/2} \sqrt{(2j+1)(2j'+1)} \times \begin{pmatrix} j & k & j' \\ \frac{1}{2} & 0 & -\frac{1}{2} \end{pmatrix} \pi(l, k, l'), \quad (27)$$

$$\pi(l_1, l_2, l_3) = \begin{cases} 1 & \text{if } l_1 + l_2 + l_3 \text{ even} \\ 0 & \text{otherwise} \end{cases}, \quad (28)$$

and the radial functions are given by

$$[r^k]_{\kappa\kappa'} = \int r^k (P_\kappa Q_{\kappa'} + Q_\kappa P_{\kappa'}) dr, \quad (29)$$

$$\langle r^k \rangle_{\kappa\kappa'} = \int r^k (P_\kappa P_{\kappa'} + Q_\kappa Q_{\kappa'}) dr. \quad (30)$$

From the angular functions it is obvious that there is no contribution from closed shells in first-order perturbation calculations. Second-order effects such as the diamagnetic corrections¹⁷ and the Sternheimer shieldings¹¹ are not considered here. We note that second-order hfs corrections which arise from the nondiagonal terms $W(J, J') = \langle JFM_F | H_{\text{hfs}} | J'FM_F \rangle$ can be calculated in the MCDF approach in much the same way as the diagonal first-order hfs terms are calculated. A MCDF study of the second-order hfs for the Li^- ion has been reported before.¹⁸ In our present case, however, we neglect the second-order hfs corrections as they are very small in size due to the large fine-structure splittings compared to the hyperfine splittings.

III. COMPARISON OF MCDF AND EXPERIMENTAL RESULTS

Table I lists the experimental and MCDF values for the excitation energies, g values, and hfs constants of low-

TABLE I. Comparison of MCDF values of the excitation energy E (in cm^{-1}), g factor g_J , and hfs constants A and B (in MHz) with experimental values for $4f^N 6s^2$ configurations. The difference between theory and experiment (MCDF—Expt.) in percent is given by Δ . The MCDF A values assume the measured values of the nuclear dipole moments. The first MCDF B value given uses the nuclear quadrupole moment value Q_{hfs} that leads to best-fit agreement with the measured hfs B 's. For some atoms the true Q value is known (through muonic-atom hfs or Coulomb-excitation studies) and it is used to calculate a second MCDF B value which is listed below the best-fit value. The typically 30% difference is consistent with a Sternheimer shielding factor of $R_{4f} = +0.23$. The information on nuclear moment values is summarized in Table II.

Atom	Configuration	Label	Observable	Expt.	MCDF	Δ (%)		
^{141}Pr	$4f^3 6s^2$	$^4I_{9/2}$	E	0.00	(0.00)	(0.0)		
			g_J	0.731 06 ^a	0.729 19	-0.26		
			A	926.209 ^{a,b}	959.80 ^c	+ 3.6		
			B	-11.878 ^{a,b}	-12.206 ^d	+ 2.8		
		$^4I_{11/2}$	E	1376.60 ^e	1265.49	-8.1		
			g_J	0.965 13 ^a	0.965 00	-0.01		
			A	730.393 ^{a,b}	758.61 ^c	+ 3.9		
			B	-11.877 ^{a,b}	-11.909 ^d	+ 0.3		
		$^4I_{13/2}$	E	2846.75 ^e	2676.49	-6.0		
			g_J	1.106 38 ^a	1.106 91	+ 0.05		
			A	613.240 ^{a,b}	636.54 ^c	+ 3.8		
			B	-12.850 ^{a,b}	-12.716 ^d	-1.0		
		$^4I_{15/2}$	E	4381.10 ^e	4202.50	-4.1		
			g_J	1.197 99 ^a	1.198 93	+ 0.08		
			A	541.575 ^{a,b}	560.15 ^c	+ 3.4		
			B	-14.558 ^{a,b}	-14.371 ^d	-1.3		
^{143}Nd	$4f^4 6s^2$	5I_4	E	0.000	(0.000)	(0.0)		
			g_J	0.603 29 ^{f,g}	0.601 38	-0.32		
			A	-195.652 ^{f,h}	-205.28 ^c	+ 4.9		
			B	122.595 ^{f,h}	120.91 ^d	-1.4		
		5I_5	E	1128.056 ^e	1038.773	-7.9		
			g_J	0.900 47 ^{f,g}	0.900 07	-0.04		
			A	-153.679 ^f	-161.28 ^c	+ 4.9		
			B	115.743 ^f	115.20 ^d	-0.5		
		5I_6	E	2366.597 ^e	2227.887	-5.9		
			g_J	1.069 91 ^f	1.070 48	+ 0.05		
			A	-130.611 ^f	-137.05 ^c	+ 4.9		
			B	119.291 ^f	119.82 ^d	+ 0.4		
		5I_7	E	3681.696 ^e	3537.273	-3.9		
			g_J	1.175 38 ^f	1.176 66	+ 0.11		
			A	-117.604 ^f	-123.33 ^c	+ 4.9		
			B	129.291 ^f	130.34 ^d	+ 0.8		
		5I_8	E	5048.602 ^e	4925.230	-2.4		
			g_J	1.245 27 ^f	1.247 05	+ 0.14		
			A	-110.476 ^f	-115.78 ^c	+ 4.8		
			B	143.952 ^f	144.41 ^d	+ 0.3		
		^{147}Sm	$4f^6 6s^2$	7F_0	E	0.00	(0.00)	(0.0)
					g_J			
				7F_1	E	292.58 ^c	237.03	-19.0
					g_J	1.498 39 ^{i,j,k}	1.499 20	+ 0.05
A	-33.493 ^{i,j,k}				-33.77 ^c	+ 0.8		
B	-58.688 ^{i,j,k}				-58.88 ^d	+ 0.3		
7F_2	E			811.92 ^c	693.54	-14.6		
	g_J			1.497 79 ^{i,j,k}	1.498 87	+ 0.07		
	A			-41.186 ^{i,j,k}	-40.71 ^c	-1.2		
	B			-62.229 ^{i,j,k}	-62.33 ^d	+ 0.2		
7F_3	E			1489.55 ^c	1327.82	-10.9		
	g_J			1.497 07 ^{i,j,k}	1.498 43	+ 0.09		

TABLE I. (Continued).

Atom	Configuration	Label	Observable	Expt.	MCDF	Δ (%)			
			<i>A</i>	-50.243 ^{i,j,k}	-49.56 ^c	-1.4			
			<i>B</i>	-33.668 ^{i,j,k}	-33.66 ^d	-0.0			
			⁷ F ₄	<i>E</i>	2273.09 ^e	2100.37	-7.6		
				<i>g_J</i>	1.496 25 ^{i,j,k}	1.497 90	+ 0.11		
				<i>A</i>	-59.707 ^{i,j,k}	-59.41 ^c	-0.5		
				<i>B</i>	21.241 ^{i,j,k}	21.48 ^d	+ 1.1		
			⁷ F ₅	<i>E</i>	3125.46 ^e	2969.50	-5.0		
				<i>g_J</i>	1.495 32 ^{i,k}	1.497 22	+ 0.13		
				<i>A</i>	-69.136 ^{i,k}	-69.61 ^c	+ 0.7		
				<i>B</i>	100.608 ^{i,k}	101.02 ^d	+ 0.4		
			⁷ F ₆	<i>E</i>	4020.66 ^e	3884.71	-3.4		
				<i>g_J</i>	1.494 17 ⁱ	1.496 31	+ 0.14		
				<i>A</i>	-78.360 ⁱ	-79.70 ^c	+ 1.7		
				<i>B</i>	203.373 ⁱ	203.06 ^d	-0.2		
			¹⁵¹ Eu	4f ⁷ 6s ²	⁸ S _{7/2}	<i>E</i>	0.00	(0.00)	(0.0)
						<i>g_J</i>	1.9935 ⁱ	1.996 29	+ 0.14
						<i>A</i>	-20.052 ^{l,b}	-19.158 ^c	-4.5
						<i>B</i>	-0.701 ^{l,b}	(-0.701) ^d	(0.0)
		-0.786 ^m				+ 12.1			
¹⁵⁹ Tb	4f ⁹ 6s ²	⁶ H _{15/2}	<i>E</i>	0.000	(0.00)	(0.0)			
			<i>g_J</i>	1.325 13 ⁿ	1.326 88	+ 0.13			
			<i>A</i>	673.753 ^{n,b}	738.57 ^c	+ 9.6			
			<i>B</i>	1449.330 ^{n,b}	1451.54 ^d	+ 0.2			
		⁶ H _{13/2}	<i>E</i>	2771.675 ^e	2583.22	-6.8			
			<i>g_J</i>	1.276 25 ⁿ	1.277 49	+ 0.10			
			<i>A</i>	682.911 ^{n,b}	750.44 ^c	+ 9.9			
			<i>B</i>	1167.489 ^{n,b}	1170.14 ^d	+ 0.2			
					1504.92 ^m	+ 28.9			
		⁶ H _{11/2}	<i>E</i>	4670.455 ^e	4475.09	-4.2			
			<i>g_J</i>		1.201 13				
			<i>A</i>	728.998 ^o	799.00 ^c	+ 9.6			
			<i>B</i>	967.997 ^o	961.43 ^d	-0.7			
		⁶ H _{9/2}	<i>E</i>	6174.925 ^e	5906.06	-4.4			
			<i>g_J</i>		1.071 61				
			<i>A</i>		907.70 ^c				
			<i>B</i>		801.94 ^d				
					1031.38 ^m				
		⁶ H _{7/2}	<i>E</i>		6988.07				
			<i>g_J</i>		0.830 42				
			<i>A</i>		1139.43 ^c				
			<i>B</i>		754.29 ^d				
		⁶ H _{5/2}	<i>E</i>		970.10 ^m				
			<i>E</i>		7780.38				
<i>g_J</i>			0.298 43						
<i>A</i>			1676.93 ^c						
<i>B</i>			881.98 ^d						
¹⁶¹ Dy	4f ¹⁰ 6s ²	⁵ I ₈	<i>E</i>	0.00	(0.00)	(0.0)			
			<i>g_J</i>	1.241 60 ^{p,g}	1.243 13	+ 0.12			
			<i>A</i>	-116.231 ^{p,b}	-122.93 ^c	+ 5.8			
			<i>B</i>	1091.577 ^{p,b}	1099.80 ^d	+ 0.8			

TABLE I. (Continued).

Atom	Configuration	Label	Observable	Expt.	MCDF	Δ (%)
					1439.54 ^m	+ 31.9
		5I_7	<i>E</i>	4134.23 ^e	3829.83	- 7.4
			<i>gJ</i>	1.173 46 ^p	1.174 46	+ 0.09
			<i>A</i>	- 126.787 ^{p,b}	- 133.99 ^c	+ 5.7
			<i>B</i>	1009.742 ^{p,b}	1015.02 ^d	+ 0.5
					1328.55 ^m	+ 31.6
		5I_6	<i>E</i>	7050.61 ^e	6691.78	- 5.1
			<i>gJ</i>	1.071 55 ^p	1.071 04	- 0.05
			<i>A</i>	- 139.635 ^o	- 148.42 ^c	+ 6.3
			<i>B</i>	960.889 ^o	954.32 ^d	- 0.7
					1249.11 ^m	+ 30.0
		5I_5	<i>E</i>	9211.58 ^e	8862.39	- 3.8
			<i>gJ</i>		0.904 93	
			<i>A</i>	- 161.971 ^o	- 173.40 ^c	+ 7.1
			<i>B</i>	894.027 ^o	906.85 ^d	+ 1.4
					1186.98 ^m	+ 32.8
		5I_4	<i>E</i>	10 925.25 ^e	10 534.78	- 3.6
			<i>gJ</i>		0.611 37	
			<i>A</i>	- 205.340 ^o	- 220.38 ^c	+ 7.3
			<i>B</i>	961.156 ^o	940.14 ^d	- 2.2
					1230.55 ^m	+ 28.0
^{165}Ho	$4f^{11}6s^2$	$^4I_{15/2}$	<i>E</i>	0.00	(0.00)	(0.0)
			<i>gJ</i>	1.195 15 ^q	1.196 46	+ 0.11
			<i>A</i>	800.583 ^q	836.77 ^c	+ 4.5
			<i>B</i>	- 1668.089 ^q	- 1621.87 ^d	- 2.8
		$^4I_{13/2}$	<i>E</i>	5419.70 ^e	5069.86	- 6.5
			<i>gJ</i>	1.104 89 ^q	1.105 71	+ 0.07
			<i>A</i>	937.209 ^q	977.91 ^c	+ 4.3
			<i>B</i>	- 1438.065 ^q	- 1409.93 ^d	- 2.0
		$^4I_{11/2}$	<i>E</i>	8605.16 ^e	8440.99	- 1.9
			<i>gJ</i>	0.982 93 ^q	0.975 63	- 0.74
			<i>A</i>	1035.140 ^q	1101.13 ^c	+ 6.4
			<i>B</i>	- 1052.556 ^q	- 1152.04 ^d	+ 9.5
		$^4I_{9/2}$	<i>E</i>	10 695.75 ^e	10 874.97	+ 1.7
			<i>gJ</i>	0.857 69 ^q	0.769 32	- 10.3
			<i>A</i>	1137.700 ^r	1309.37 ^c	+ 15.1
			<i>B</i>	- 494.482 ^r	- 1070.64 ^d	+ 116.5
^{167}Er	$4f^{12}6s^2$	3H_6	<i>E</i>	0.000	(0.00)	0.0
			<i>gJ</i>	1.163 80 ^s	1.164 76	+ 0.08
			<i>A</i>	- 120.487 ^{t,u}	- 123.60 ^c	+ 2.6
			<i>B</i>	- 4552.984 ^{t,u}	- 4642.02 ^d	+ 2.0
					- 5883.02 ^m	+ 29.2
		3H_5	<i>E</i>	6958.329 ^e	6654.47	- 4.4
			<i>gJ</i>		1.032 13	
			<i>A</i>	- 159.522 ^t	- 163.63 ^c	+ 2.6
			<i>B</i>	- 4119.767 ^t	- 4221.76 ^d	+ 2.5
					- 5350.42 ^m	+ 29.9
		3H_4	<i>E</i>	10 750.982 ^e	11 054.94	+ 2.8
			<i>gJ</i>		0.967 63	
			<i>A</i>	- 173.431 ^t	- 175.17 ^c	+ 1.0
			<i>B</i>	- 2429.382 ^t	- 2173.15 ^d	- 10.5
					- 2754.13 ^m	+ 13.4
		3F_4	<i>E</i>	5035.193 ^e	6178.21	+ 22.7

TABLE I. (Continued).

Atom	Configuration	Label	Observable	Expt.	MCDF	Δ (%)
			g_J		1.100 74	
			A	-121.840 ^t	-127.77 ^t	+ 4.9
			B	518.628 ^t	2.01 ^d	-99.6
					2.55 ^m	-99.5
		3F_3	E	12 377.534 ^e	14 024.43	+ 13.3
			g_J		1.082 25	
			A	-143.489 ^t	-144.80 ^e	+ 0.9
			B	1238.415 ^t	1252.82 ^d	+ 1.2
					1587.75 ^m	+ 28.2
		3F_2	E	13 097.906 ^e	15 413.70	+ 17.7
			g_J		0.712 55	
			A	-167.147 ^t	-175.53 ^e	+ 5.0
			B	1686.564 ^t	1481.28 ^d	-12.2
					1877.29 ^m	+ 11.3
^{169}Tm	$4f^{13}6s^2$	$^2F_{7/2}$	E	0.000	(0.00)	(0.0)
			g_J	1.141 19 ^{v,w}	1.141 85	+ 0.06
			A	-374.138 ^{v,w,b}	-376.79 ^e	+ 0.7
			B			
		$^2F_{5/2}$	E	8771.243 ^e	8563.90	-2.4
			g_J		0.855 45	
			A	-704.649 ^o	-708.43 ^e	+ 0.5
			B			

^aSee Ref. 19.^bSee Ref. 1.^cSee Ref. 20.^dSee Ref. 21.^eSee Ref. 4.^fSee Ref. 22.^gSee Ref. 23.^hSee Ref. 24.ⁱSee Ref. 25.^jSee Ref. 26.^kSee Ref. 27.^lSee Ref. 28.^mSee Ref. 29.ⁿSee Ref. 30.^oSee Ref. 31.^pSee Ref. 32.^qSee Ref. 33.^rSee Ref. 34.^sSee Ref. 35.^tSee Ref. 36.^uSee Ref. 37.^vSee Ref. 38.^wSee Ref. 39.

lying $4f^N6s^2$ states of neutral rare-earth atoms. The atom, with its nuclear mass number, is identified in the first column, and the electron configuration and atomic state are given in columns 2 and 3. The atomic state given is that of the principal component of the eigenvector. Column 4 specifies the particular observable for which data are given in columns 5, 6, and 7. The experimental values are given in column 5, the MCDF values are given in column 6, and the departure of the MCDF value from the measured value (in %) is listed in the final column. The experimental errors are not given, but are in all cases much smaller than the differences between theory and experiment. Data are given only for the lightest atom in those cases where experimental results are known for two or more odd- A isotopes.

Calculation of the MCDF values of the hfs constants A and B requires knowledge of the corresponding nuclear moments μ_I and Q . The values used for the dipole moments are the directly measured values, determined in most cases by atomic-beam triple resonance.⁴⁰ The values used are listed in Table II. Except for ^{141}Pr , they are all taken from the compilation of Fuller¹ to ensure consistency with regard to the diamagnetic shielding correction. The ^{141}Pr value is from Lew.¹⁹ The ^{159}Tb value is from

electron paramagnetic resonance;^{1,44} all the others are from atomic-beam magnetic resonance.¹

Since the spectroscopic nuclear electric-quadrupole moment is not accurately known for most nuclei, a different approach is used. For all atoms the Q value was considered unknown and adjusted to give the best least-squares fit of the MCDF to the observed B values of all members of the ground term (for ^{165}Ho the $^4I_{9/2}$ state was ignored in the fit because of the large errors in the calculated values of the observables).

In Table I this best-fit B value is given first. For some atoms the Q value has been precisely determined by muonic-x-ray hfs or Coulomb-excitation studies, thereby avoiding Sternheimer shielding effects. In these cases the true value of Q is used to produce a second MCDF B value which is listed below the least-squares-fit value in Table I. The difference of typically 30% between the two B values is a direct measure of the distortion of the electron core by the nuclear quadrupole moment (Sternheimer effect). In the usual expression the true quadrupole moment Q is expressed in terms of the apparent moment Q_{hfs} by the relation¹¹

$$Q = \frac{1}{1 - R_{nl}} Q_{\text{hfs}}. \quad (31)$$

TABLE II. Nuclear moment information for the atoms studied. Here, μ_I are the measured nuclear dipole moment values (in units of μ_N) used in the MCDF calculations of the hfs A values, and Q_{hfs} , Q_{pred} , and Q_{obs} are nuclear quadrupole moment values in barns (10^{-24} cm²). Q_{hfs} are the quadrupole moment values that, together with the MCDF radial calculations, lead to a best fit to the observed hfs B values. Q_{pred} are the quadrupole moment values predicted from the Q_{hfs} values and the assumed Sternheimer shielding factor $R_{4f} = +0.23$. Q_{obs} are the spectroscopic quadrupole moment values determined by muonic-atom hfs or Coulomb-excitation methods, and Δ are the differences between the predicted and the observed Q values ($Q_{\text{pred}} - Q_{\text{obs}}$) in percent. The discrepancy for ^{151}Eu arises from the quadrupole hfs measurement being made in an atomic S state and is discussed in the text.

Nucleus	μ_I	Q_{hfs}	Q_{pred}	Q_{obs}	Δ (%)
^{141}Pr	4.136 ^a	-0.051	-0.066		
^{143}Nd	-1.063 ^{b,c}	-0.459	-0.596		
^{147}Sm	-0.8129 ^{b,d}	-0.203	-0.263		
^{151}Eu	3.4631 ^{b,e}	0.504	(0.655)	0.561 ^{f,g}	(-17.0)
^{159}Tb	2.008 ^{b,h}	1.113	1.445	1.432 ⁱ	-0.9
^{161}Dy	-0.4792 ^{b,j}	2.017	2.619	2.64 ^k	0.8
^{165}Ho	4.125 ^{b,l}	2.596	3.371	3.57 ^m	5.6
^{167}Er	-0.5647 ^{b,c}	2.817	3.658	3.565 ⁱ	-2.6
^{169}Tm	-0.2310 ^{b,n}				

^aSee Ref. 19.

^bSee Ref. 1.

^cSee Ref. 36.

^dSee Ref. 26.

^eSee Ref. 41.

^fSee Ref. 42.

^gSee Ref. 43.

^hSee Ref. 44.

ⁱSee Ref. 45.

^jSee Ref. 46.

^kSee Ref. 47.

^lSee Ref. 48.

^mSee Ref. 49.

ⁿSee Ref. 39.

Since the B values are proportional to the Q values, this may be modified to read

$$B = \frac{1}{1 - R_{nl}} B_{\text{hfs}} \quad (32)$$

In this expression, B_{hfs} is the B value inferred from atomic hfs (listed first for each atom in Table I), while B is the value (listed below B_{hfs} , or omitted if unavailable) calculated from the true value of Q . The 30% difference is consistent with $R_{4f} = +0.23$ as found by Childs and Cheng.⁵⁰ Table II gives Q_{hfs} (column 3), the predicted (true) Q value determined by letting $R_{4f} = +0.23$ (column 4), and the measured value of Q (column 5). The agreement between columns 4 and 5 is excellent for ^{159}Tb , ^{161}Dy , ^{165}Ho , and ^{167}Er . The poor agreement for ^{151}Eu presumably arises from the difficulties, both experimental and theoretical, of evaluating the (nuclear) quadrupole moment in a rather pure (atomic) S state for which the extremely small quadrupole hfs arises only through departure from L - S coupling. If the eigenvector picks up some non- $4f$ character, the appropriate Sternheimer factor may deviate from $R_{4f} = 0.23$ and the predicted Q values would be different from that listed in column 4 of Table II. In view of these uncertainties the apparent 17% discrepancy for ^{151}Eu is not surprising and the relevant entries in Table II are put in parentheses.

In general, we see from Table I that the agreement between the MCDF values and the measured values is extremely good in spite of the lack of adjustable parameters. The excitation energies are predicted to typically 6%, the g values to 0.1%, the A values to 5%, and the B values within 2% (not counting the 30% Sternheimer effect which is omitted in the MCDF treatment).

The J dependence of the calculated values is also rather

good. Thus, for example, the range in the ^{147}Sm B values from -58 (7F_1) to $+203$ MHz (7F_6) is accurately predicted by the MCDF theory. For the same atom, the L - S -coupling model predicts $g_J = 1.50116$ independent of J , but a small J dependence results from state-dependent admixtures. The J dependence of the calculated g values is in good qualitative agreement with experiment as shown in Fig. 1. Residual discrepancies presumably are due to the diamagnetic corrections¹⁷ which are second-order effects and are not included in this calcula-

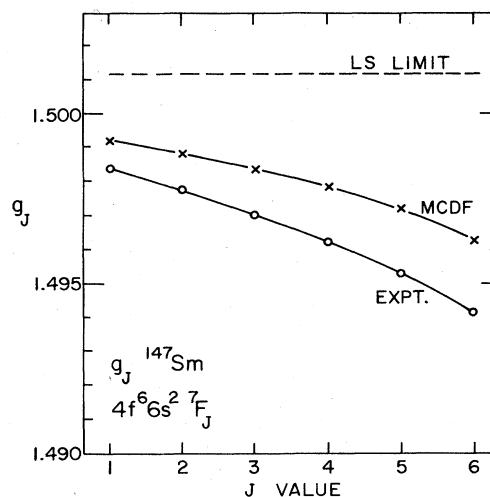


FIG. 1. J dependence of the Landé g factor in the $4f^6 6s^2 7F_J$ ground term of ^{147}Sm . State-dependent admixtures perturb the L - S -limit prediction $g_J = 1.50116$ for all J . The observed J dependence is reproduced qualitatively by the MCDF theory.

tion. If the corrections calculated in Ref. 17 are applied to our MCDF values in Fig. 1, the agreement with the experiment is dramatically improved. Unfortunately, however, the authors did not list the diamagnetic corrections separately from the relativistic corrections already included in our MCDF results.

The MCDF results do not, of course, reproduce the experimental results perfectly. From Table I we see that the MCDF excitation energies are too small in every case except for the $^4I_{9/2}$ state of ^{165}Ho and for the higher excited states of ^{167}Er . The region of poorest agreement between theory and experiment is near the end of the shell at high excitation; this is exactly where state mixing is most critical. The g values and hfs constants are also calculated less accurately in this region, clearly indicating that configuration interactions are stronger for these states. In an effort to improve the MCDF results for the excited levels of ^{167}Er , the basis set was greatly expanded to include the $4f^{12}6s5d$, $4f^{11}6p6s^2$, and $4f^{12}6p^2$ configurations. The use of such expanded basis sets did not significantly improve the agreement with experiment for any of the observables, and it is of the greatest interest to understand why. At this point, it is not even clear whether the absence of as yet unidentified key configurations is the source of the discrepancies or whether the problem is more fundamental. It is hoped that this paper will serve to stimulate further work in this area.

The calculated A values are too large in most cases but are very close (typically within 1%) to the measured values in ^{147}Sm even though the calculated energies for these same states are much further from experiment than those for any other atom studied. It is worth noting that eigenvectors that are excellent for reproducing experimental values of the hfs constants may not be as good for predicting the excitation energies, and vice versa.

IV. CONCLUSIONS

The MCDF theory has been used to calculate the excitation energy, g value, and hfs constants for all levels within the ground $4f^N6s^2$ multiplets of the neutral rare-earth atoms. The j - j configurations included are limited, except as mentioned below, to those necessary to reproduce the $4f^N6s^2$ configurations. Except for this truncation, however, there is no arbitrariness or adjustability in the theory; all the results follow directly from first principles (the nuclear moments are taken from experiment).

In comparing the calculated values with the experimental ones (many of which have been obtained only within the last two years), one typically finds agreement for the excitation energies and hfs A values to about 5%; the cal-

culated excitation energies are in most cases too small and the A values too large. That the calculated g values agree with experiment to about 0.1% is not very surprising, as they are relatively insensitive to changes in the wave functions.

For those atoms for which the nuclear quadrupole moment is accurately known one finds the calculated hfs B values are about $(30 \pm 2)\%$ too large. This is a direct measure of the Sternheimer shielding and is not taken into account in the MCDF calculations. On the assumption that the shielding factor R_{4f} is constant throughout the $4f$ shell (as it appears to be),⁵⁰ the "true" quadrupole moment is predicted (Table II, column 4) for each of several nuclei for which there are as yet no measurements. New measurements to test these predictions would be of great interest.

As the relativistic effects are included nonperturbatively, the J dependence of the MCDF results is remarkably close to the observed for all four observables (E , g , A , and B) studied. This gives considerable confidence in the way the theory predicts L - S -state admixture and greatly simplifies the calculations of spin-orbit corrections.

In view of the limited basis set chosen, the high order of agreement between theory and experiment is remarkable. The region of poorest agreement with experiment is near the end of the shell at high excitation energy. This is presumably due to stronger electron correlation effects in more-than-half-filled shells. These difficulties are well illustrated by the data for the $^4I_{11/2,9/2}$ levels of ^{165}Ho and the 3H_4 and 3F_4 levels of ^{167}Er . It appears that a few key configurations are missing in our calculations; whether they involve inner-shell vacancies (core polarization) or only outer electrons is not clear, although semiempirical calculations have suggested³¹ that core polarization plays only a very minor role in the hfs of $4f^N6s^2$ configurations. Identification of these configurations in future MCDF studies will certainly enhance our understandings of electron correlations for rare-earth atoms.

Considerable experimental data exists for more complex electron configurations of the rare earths and may well provide a useful subject for subsequent studies. In most cases the states involved are more highly excited than the $4f^N6s^2$ levels considered here, and the greater admixtures expected would present a still more challenging test of the *ab initio* theory.

ACKNOWLEDGMENTS

This research was supported by the U. S. Department of Energy (Office of Basic Energy Sciences), under Contract No. W-31-109-Eng-38.

¹The results of this work are summarized in G. H. Fuller, J. Phys. Chem. Ref. Data 5, 835 (1976).

²No compilation of this work has yet appeared; papers relating to specific atoms are cited individually below.

³S. D. Rosner, T. D. Gaily, and R. A. Holt, Phys. Rev. Lett. 40, 851 (1978); W. Ertmer and B. Hofer, Z. Phys. A 276, 9 (1976).

⁴The low-lying states of the neutral rare-earth atoms are con-

veniently tabulated in *Atomic Energy Levels*, edited by W. C. Martin, R. Zalubas, and L. Hagan, Natl. Bur. Stand. Ref. Data Ser., Natl. Bur. Stand. (U.S.) Circ. No. 60 (U.S. GPO, Washington, D.C., 1978).

⁵A good paper of this type is J. F. Wyart and P. Camus, Physica (Utrecht) 93C, 227 (1978).

⁶P. G. H. Sandars and J. Beck, Proc. R. Soc. London, Ser. A

- 289, 97 (1965).
- ⁷See, for example, I. Lindgren and A. Rosén, *Case Stud. At. Phys.* **4**, 93 (1974); **4**, 197 (1974).
- ⁸W. J. Childs, *Case Stud. At. Phys.* **3**, 215 (1973).
- ⁹See, for example, R. Glass, *J. Phys. B* **11**, 3459 (1978).
- ¹⁰See, for example, I. Lindgren and J. Morrison, *Atomic Many-Body Theory* (Springer, Berlin, 1983), Chap. 14.
- ¹¹R. M. Sternheimer, *Phys. Rev.* **146**, 140 (1966); **164**, 10 (1967).
- ¹²J. P. Desclaux, *Comput. Phys. Commun.* **9**, 31 (1974).
- ¹³A. J. Akhiezer and V. B. Berestetskii, *Quantum Electrodynamics* (Interscience, New York, 1965), Chap. 1, Sec. 4.2.
- ¹⁴L. Armstrong, Jr., *Theory of the Hyperfine Structure of Free Atoms* (Wiley-Interscience, New York, 1971), Chap. 6, Sec. 1.
- ¹⁵M. E. Rose, *Elementary Theory of Angular Momentum* (Wiley, New York, 1957), Chap. 5, Sec. 20.
- ¹⁶Reference 13, Chap. 8, Sec. 50.2.
- ¹⁷B. R. Judd and I. Lindgren, *Phys. Rev.* **122**, 1802 (1961).
- ¹⁸K. T. Cheng, J. E. Hardis, E. J. Dehm, and D. R. Beck, *Phys. Rev. A* **30**, 698 (1984).
- ¹⁹H. Lew, *Bull. Am. Phys. Soc.* **15**, 795 (1970).
- ²⁰The MCDF calculation assumes the accepted measured value for μ_f . (See Table II, column 2.)
- ²¹The MCDF calculation adjusts Q_{hfs} to achieve a best least-squares fit to the measured B values. (See Table II, column 3.)
- ²²W. J. Childs and L. S. Goodman, *Phys. Rev. A* **6**, 1772 (1972).
- ²³K. F. Smith and I. J. Spalding, *Proc. R. Soc. London, Ser. A* **265**, 133 (1961).
- ²⁴I. J. Spalding, *Proc. Phys. Soc. London* **81**, 156 (1963).
- ²⁵W. J. Childs and L. S. Goodman, *Phys. Rev. A* **6**, 2011 (1972).
- ²⁶G. K. Woodgate, *Proc. R. Soc. London, Ser. A* **293**, 117 (1966).
- ²⁷R. G. H. Robertson, J. C. Waddington, and R. G. Summers-Gill, *Can. J. Phys.* **46**, 2499 (1968).
- ²⁸P. G. H. Sandars and G. K. Woodgate, *Proc. R. Soc. London, Ser. A* **257**, 269 (1960).
- ²⁹The MCDF calculation assumes Q value measured in muonic atom or by Coulomb excitation. (See Table II, column 5).
- ³⁰W. J. Childs, *Phys. Rev. A* **2**, 316 (1970).
- ³¹W. J. Childs, H. Crosswhite, L. S. Goodman, and V. Pfeufer, *J. Opt. Soc. Am. B* **1**, 22 (1984).
- ³²W. J. Childs, *Phys. Rev. A* **2**, 1692 (1970).
- ³³B. Burghardt, S. Büttgenbach, N. Glaeser, R. Harzer, G. Meisel, B. Roski, and F. Traber, *Z. Phys. A* **307**, 193 (1982).
- ³⁴W. J. Childs, D. R. Cok, and L. S. Goodman, *J. Opt. Soc. Am.* **73**, 151 (1983).
- ³⁵J. G. Conway and B. G. Wybourne, *Phys. Rev.* **130**, 2325 (1963).
- ³⁶W. J. Childs, L. S. Goodman, and V. Pfeufer, *Phys. Rev. A* **28**, 3402 (1983).
- ³⁷K. F. Smith and P. J. Unsworth, *Proc. Phys. Soc. London* **86**, 1249 (1965).
- ³⁸G. J. Ritter, *Phys. Rev.* **128**, 2238 (1962).
- ³⁹D. Gliglberger and S. Penselin, *Z. Phys.* **199**, 244 (1967).
- ⁴⁰This method is described, for example, in Ref. 8, p. 252.
- ⁴¹L. Evans, P. G. H. Sandars, and G. K. Woodgate, *Proc. R. Soc. London, Ser. A* **289**, 114 (1965).
- ⁴²R. A. Carrigan, Jr., P. D. Gupta, R. B. Sutton, M. N. Suzuki, A. C. Thompson, R. E. Coté, W. V. Prestwich, A. K. Gaigalas, and S. Raboy, *Phys. Rev. Lett.* **20**, 874 (1968).
- ⁴³K. E. G. Löbner, M. Vetter, and V. Hönig, *Nucl. Data Tables A7*, 495 (1970). The intrinsic moments listed are transformed to spectroscopic moments for use in the present study.
- ⁴⁴J. M. Baker, J. R. Chadwick, G. Garton, and J. P. Hurrell, *Proc. R. Soc. London, Ser. A* **286**, 352 (1965).
- ⁴⁵Y. Tanaka, R. M. Steffen, E. B. Shera, W. Reuter, and M. V. Hoehn, *Phys. Rev. Lett.* **51**, 1633 (1983).
- ⁴⁶J. Ferch, thesis, University of Bonn, 1972, as quoted by A. Rosén and H. Nyquist, *Phys. Scr.* **6**, 24 (1972).
- ⁴⁷B. Elbek, K. O. Nielsen, and M. C. Oesen, *Phys. Rev.* **108**, 406 (1957).
- ⁴⁸R. A. Haberstroh, T. I. Moran, and S. Penselin, *Z. Phys.* **252**, 421 (1972).
- ⁴⁹M. C. Olesen and B. Elbek, *Nucl. Phys.* **15**, 134 (1960).
- ⁵⁰W. J. Childs and K. T. Cheng, *Phys. Rev. A* **30**, 677 (1984).